

Motivic analysis of neuronal responses to visual stimuli

A Project Report

submitted by

ATHUL VIJAYAN

*in partial fulfilment of the requirements
for the award of the degree of*

MASTER OF TECHNOLOGY



**DEPARTMENT OF ENGINEERING DESIGN
INDIAN INSTITUTE OF TECHNOLOGY, MADRAS.**

April 2016

THESIS CERTIFICATE

This is to certify that the thesis entitled **Motivic analysis of neuronal responses to visual stimuli**, submitted by **Athul Vijayan**, to the Indian Institute of Technology, Madras, for the award of the degree of **Master of Technology**, is a bona fide record of the research work carried out by him under my supervision. The contents of this thesis, in full or in parts, have not been submitted to any other Institute or University for the award of any degree or diploma.

Dr. Hema A. Murthy
Research Guide
Assistant Professor
Dept. of Computer Science and Engineering
IIT-Madras, 600 036

Place: Chennai

Date:

ACKNOWLEDGEMENTS

**I would like to thank everyone who helped me.

ABSTRACT

KEYWORDS: Markov Decision Processes, Symmetries, Abstraction

TABLE OF CONTENTS

ACKNOWLEDGEMENTS	i
ABSTRACT	ii
LIST OF TABLES	v
LIST OF FIGURES	vii
ABBREVIATIONS	viii
NOTATION	ix
1 Introduction	1
2 Background and Previous work	2
2.1 Visual pathway in brain	2
2.1.1 Neurons	3
2.1.2 Visual pathway	4
2.2 Experiment setup	6
2.2.1 Sinusoidal grating visual stimuli	7
2.2.2 Natural videos visual stimuli	7
2.3 Previous works	7
3 Analyzing neuronal properties	8
3.1 Quantifying Orientation and Directional selectivity	8
3.2 Modeling neuronal response	11
3.3 Finding similarly tuned neurons	12
3.4 Study of principal components	14
3.5 Study of Reliability	16

4	Searching for Motifs	18
4.1	Cross-Correlation Function	19
4.2	ACFGram	21
5	Rough Longest Common Subsequence (RLCS)	24
5.1	Longest Common Subsequence (LCS)	24
5.2	RLCS	25
5.2.1	Motivic analysis of Neuronal signals with RLCS	29
5.2.2	Normalized RLCS score as a correlation measure	34
6	Inferences and Future work	36
A	More RLCS plots	37

LIST OF TABLES

5.1 Some examples of LCS in string comparison	25
---	----

LIST OF FIGURES

3.1 Responses $R(\theta_k)$ of a simple neuron for each θ_k plotted in both orientation and direction space. Equal lobes in direction space shows direction is irrelevant.	9
3.2 Responses $R(\theta_k)$ of a complex neuron for each θ_k plotted in both orientation and direction space. Unequal lobes in direction space shows one direction is preferred than its opposite.	10
3.3 Responses $R(\theta_k)$ of a an orientation insensitive neuron for each θ_k plotted in both orientation and direction space. Similar responses to all orientations shows absence of selectivity.	10
3.4 Fit of orientation and direction tuning curves of a neuron. The distinct peak in the orientation tuning curve shows selectivity to orientation θ_{pref} . Different σ_1 and σ_2 in direction tuning curve shows direction sensitive cell. - Thus a complex cell	12
3.5 Fit of orientation and direction tuning curves of a neuron. The distinct peak in the orientation tuning curve shows selectivity to orientation θ_{pref} . Similar σ_1 and σ_2 in direction tuning curve direction of stimuli is irrelevant. - Thus a simple cell	13
3.6 Pairwise Pearson correlation of neurons. Both axes are sorted in decreasing order of OSI.	14
3.7 Orientation tuning curves of some neurons retrieved from correlation study. All of them have a same preferred orientation.	15
3.8 Principal Component Analysis of response of neuron to drifting sinusoidal grating stimuli.	16
3.9 Reliability measure R_A for different neurons	17
4.1 Cross-Correlation function between a target neuron response and a manually chosen subsequence from template neuron.	20
4.2 Extracting frame from template based on frame width and ending.	21
4.3 ACFGram plots for template and target responses from same neuron.	22
4.4 ACFGram plots for template and target responses from different neurons.	23

5.1	Score matrix from RLCS of responses a neuron to different trials. .	30
5.2	Extracted motif (longest) from responses a neuron to different trials.	31
5.3	Score matrix from RLCS of responses of two neurons in a mouse.	32
5.4	Extracted motif (longest) from responses of two neurons in a mouse.	32
5.5	Score matrix from RLCS of responses of two neurons in a mouse.	33
5.6	Extracted motif (longest) from responses of two neurons in a mouse.	34
5.7	Demonstration of RLCS score's dominance over Pearson correlation as a metric of similarity. RLCS analysis of two signals having low Pearson correlation. Extracted common subsequence was not detected by Pearson correlation.	35

ABBREVIATIONS

RLCS	Rough Longest Common Subsequence
LCSS	Longest Common Segment Set

NOTATION

$\rho(a, b)$	Pearson correlation between a and b
V1	Primary Visual Cortex

CHAPTER 1

Introduction

CHAPTER 2

Background and Previous work

Signal processing and machine learning methods are great to bring out valuable inferences from data. The conclusions we draw from statistical methods will have meaning only with the context of the problem. To analyze and draw conclusions from neuronal data, we need to have a good understanding of the background. This chapter provides background in basic Neuroscience and previous works in the similar problem.

2.1 Visual pathway in brain

Brain is the most sophisticated organ nature has devised. Brain is mainly made up of orderly arrays of cells called neuron (also called nerve cell). Neurons are electrically excitable cells which process information through electrical and chemical processes. Neurons are also information carriers that connects the whole body to the brain. Visual perception is a complex function yet brain does it very efficiently. There are 100 million photo-receptors in a human retina. But there are only nearly 1 millions axons that carry information to brain [Bear *et al.* [2007]]. Understanding how brain represents and process visual information can help us create artificially intelligent machines with vision abilities.

This section describes functioning of neurons and background on visual pathway of brain.

2.1.1 Neurons

Neurons consists of three parts - soma, dendrites and axons. Axon is the signal transmitting cylinder like nerve fiber that comes out from soma. Dendrites are branched fibers that receive information from other nerve cells. The axon can be anywhere from less than a millimeter to a meter or more in length; the dendrites are mostly in the millimeter range. Near the point where it ends, an axon usually splits into many branches, whose terminal parts come very close to but do not quite touch the cell bodies or dendrites of other nerve cells. At these regions, called synapses, information is conveyed from one nerve cell, the presynaptic cell, to the next, the postsynaptic cell [Hubel [1995]].

The job of a nerve cell is to take in information from the cells that feed into it, process that information, and to deliver the integrated information to other cells. The information is usually conveyed in the form of brief events called nerve impulses. The nerve cell is bathed in and contains salt water. Because most of the salt molecules are ionized, the fluids both inside and outside the cell will contain chloride, potassium, sodium, and calcium ions (Cl^- , K^+ , Na^+ and Ca^{2+}). In the resting state, the inside and outside of the cell differ in electrical potential by 0.07 volts. The signals that the nerve conveys consist of transient changes in this resting potential, which travel along the fiber from the cell body to the axon endings. During an impulse, a large number of sodium pores in a short length of the nerve fiber suddenly open, so that briefly the sodium ions dominate and that part of the nerve suddenly becomes negative outside, relative to inside. The sodium pores then reclose, and meanwhile even more potassium pores have opened than are open in the resting state. Both eventsthe sodium pores reclosing and additional potassium pores openinglead to the rapid restoration of

the positive-outside resting state. The whole sequence lasts about one-thousandth of a second.

Neuron's response are quantified by number of spikes per second - called spike rate. In the data we use in this work, we use Ca^{2+} concentration as the response of neuron. As the spikes are caused by the ion concentration changes, Ca^{2+} ion concentration is a good proxy for spike rate. Vogelstein deconvolution algorithm [Vogelstein *et al.* [2010]] extracts the spike train of each neuron from a raw fluorescence movie. We use inferred spike rate from Vogelstein deconvolution algorithm as the neuron's response.

2.1.2 Visual pathway

The enormous task of taking the light that gets reflected from objects around us to the two retinas and translating it into a meaningful visual scene is often ignored. The visual pathway starts with eye, of which most important part is the retina. Retina contains light receptors called rods and cones. Rods are far more numerous than cones and are responsible for our vision in dim light but do not respond to bright light. Cones do not respond to dim light but are responsible for our ability to see fine detail and for our color vision. The layer of cells at the back of the retina contains the retinal ganglion cells which then reaches brain through optic nerve. The output of the eyes are output of retinal ganglion cells rather than retina.

Receptive field refers to the specific receptors that input information into a given cell in the nervous system. For vision, it refers to a region on the retina from where information goes to a particular neuron. As we go into higher levels of brain, the receptive field gets complicated. Note that receptive fields do overlap.

The optical nerve goes to brain to join primary visual cortex through cells called lateral geniculate cells. About half the fibers coming from an eye cross to the side of the brain opposite the eye of origin, and half stay on the same side. lateral geniculate cells receive fibers from the cerebral cortex also, which plays some role in attention. The primary visual cortex (V1) is a plate of cells 2 millimeters thick, with a surface area of a few square inches. V1 contains three different kinds of cells - simple cells, complex cells and orientation insensitive cells. Like in an artificial neural network, the neurons in higher levels captures edge properties in the image. Neurons in V1 are also orientation selective cells which can represent visual information in terms of edges as visual features. [Hubel [1995]]

Neurons in V1 are selective to orientation and direction of a visually contrasting pattern in the receptive field. The orientation is the angle to which the patterns is aligned, direction is the direction in which the pattern is moving in the next frame. Figure shows the behavior of orientation selective neurons. They have a preferred orientation to which they have optimum response. As the orientation deviates from preferred orientation, the responses reduces exponentially.

Within orientation selective cells, there are two kinds of cells - simple and complex cells. Consider moving the oriented stimuli perpendicular to the orientation angle. Among the two perpendicular directions, some neurons respond to one perpendicular direction more than the other. These cells are called complex cells. Neurons which respond similarly to both directions of motion is called simple cells. The figure explains the directional sensitivity of neurons in V1.

2.2 Experiment setup

The data for this work was obtained from experiments conducted in Sur's lab of Neuroscience, MIT. A brief overview of the experiments and data is required to follow the upcoming chapters.

"Data in this study were collected from adult (> 8 weeks old) mice of either sex. Mice were anesthetized using isoflurane (3% induction, 1.52% during surgery). A custom-built metal head post was attached to the skull using dental cement (C&B-Metabond, Parkell), and a 3-mm-diameter craniotomy was performed over binocular V1 (~ 23 mm lateral and 0.5 mm anterior to lambda). Care was taken not to rupture the dura mater. The core body temperature was maintained at 37.5C using a heating blanket (Harvard Apparatus).

For awake experiments, mice were first habituated for 5 d to head fixation on a custom-built stage. Once habituated, the mice received a microinjection of 100-200 nl of AAV1.Syn.GCaMP6f.WPRE.SV40 (University of Pennsylvania Vector Core, diluted to a titer of 10^{12} genomes ml⁻¹), following which a cranial window was implanted over the craniotomy and sealed. Mice were allowed to recover for 23 weeks to allow for adequate expression of the virus before imaging commenced. Imaging was performed using a Prairie Ultima two-photon system. The imaging was done at a frequency of 20Hz. The imaging was done while mice were presented with a visual stimuli on a 23 inch gamma-corrected LCD monitor (Dell) covering a visual space of ~ 96×54 deg²." [Rikhye and Sur [2015]]

The experiment was performed for the following two sets of visual stimuli.

2.2.1 Sinusoidal grating visual stimuli

2.2.2 Natural videos visual stimuli

2.3 Previous works

CHAPTER 3

Analyzing neuronal properties

Characteristics of neurons in the V1 are discussed in the background section. In this chapter, we use experimental data to demonstrate the claimed properties of neurons in V1. In the experiment, a drifting sinusoidal grating video is shown to awake mice and neuronal responses were recorded. See Section 2.2.1 for detailed experiment setup.

Average response of a neuron is modeled as a function of orientation using a Gaussian function. Similarly, average response to various directions are modeled using a mixture of Gaussian functions. Root mean square of residuals are used as a goodness of fit measure.

Neurons in V1 are classified into simple, complex and unselective cells. Classifying a neuron into either of this class is useful as we can find the population of similar cells in the brain. Rather than thresholding OSI and DSI, We have used a k-means clustering algorithm with more features to classify cells.

3.1 Quantifying Orientation and Directional selectivity

Modern imaging technologies allow examining responses of neurons with clarity. Even though it was known that neurons in V1 are selective to orientation, we need robust metrics to quantify degree of selectivity and preferred orientation.

Plotting responses to each stimuli direction in a vector space provides an intuition about the characteristics. In orientation space, responses of two opposite directions are averaged. Angle varies from 0° to 180° in orientation space while angle angle changes from 0° to 360° in direction space. Figure** shows responses plotted in orientation and direction space for a simple neuron. Length of the vector sum is a good metric for amount of selectivity and preferred orientation. Normalized length of vector sum in orientation space is defined as OSI(Orientation Selectivity Index).

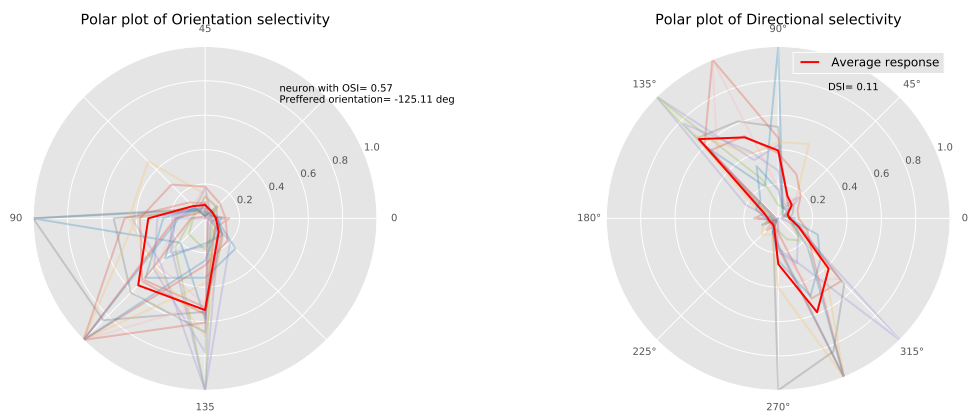
$$OSI = \left| \frac{\sum_k R(\theta_k) \exp(2i\theta_k)}{\sum_k R(\theta_k)} \right|$$

Similarly, Normalized length of vector sum in direction space is defined as DSI(Direction Selectivity Index).

$$DSI = \left| \frac{\sum_k R(\theta_k) \exp(i\theta_k)}{\sum_k R(\theta_k)} \right|$$

Where $R(\theta_k)$ is the average response to angle θ_k .

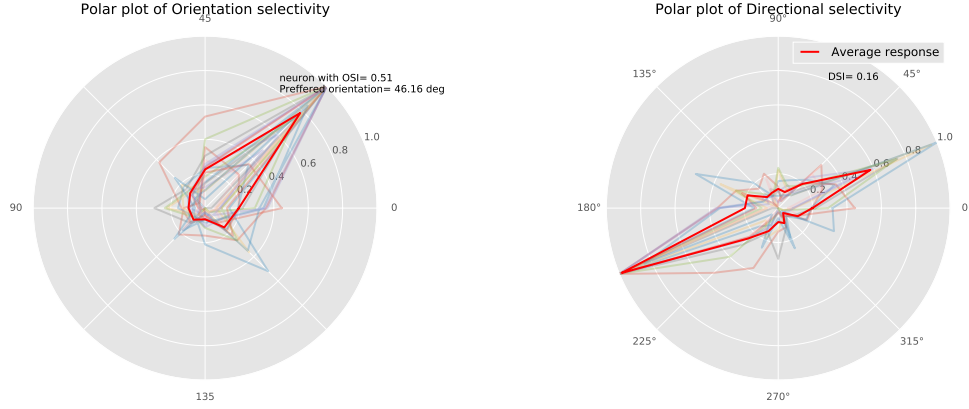
A simple neuron is expected to have high OSI but low DSI. Polar plots of responses in orientation and direction space is shown in Figure 5.7



(a) Responses plotted in orientation space (b) Responses plotted in direction space

Figure 3.1: Responses $R(\theta_k)$ of a simple neuron for each θ_k plotted in both orientation and direction space. Equal lobes in direction space shows direction is irrelevant.

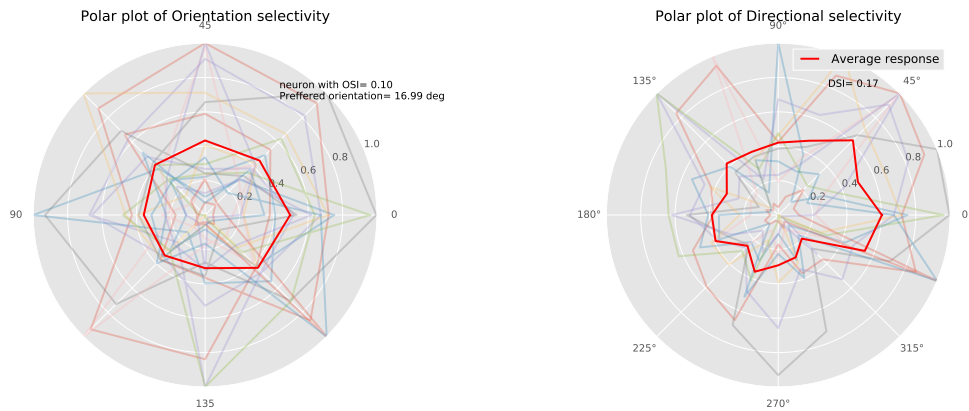
A complex neuron is expected to have high OSI and high DSI. Polar plots of responses in orientation and direction space is shown in Figure 3.2



(a) Responses plotted in orientation space (b) Responses plotted in direction space

Figure 3.2: Responses $R(\theta_k)$ of a complex neuron for each θ_k plotted in both orientation and direction space. Unequal lobes in direction space shows one direction is preferred than its opposite.

An orientation insensitive neuron is expected to have low values for both OSI and DSI. Polar plots of responses in orientation and direction space is shown in Figure 3.3.



(a) Responses plotted in orientation space (b) Responses plotted in direction space

Figure 3.3: Responses $R(\theta_k)$ of an orientation insensitive neuron for each θ_k plotted in both orientation and direction space. Similar responses to all orientations shows absence of selectivity.

3.2 Modeling neuronal response

Modeling the response of neuron to various orientations and visualizing is a great way to see if in fact there is an orientation selectivity. If the cell seems selective, we can also characterize the degree of selectivity and preferred orientation from model parameters.

Orientation tuning curve is modeled using a Gaussian function with constant offset. The empirical form of the orientation tuning curve is,

$$R_o(\theta) = C + R_p \exp \left\{ \frac{-\|\theta - \theta_{pref}\|^2}{2\sigma^2} \right\}$$

Where $R_o(\theta)$ is the time-averaged response of neuron to angle of orientation θ . Parameter θ_{pref} is the preferred orientation of the neuron. Tuning width σ tell us how much the cell is selective. C is a constant offset.

Similarly, we can model direction tuning curve using a mixture of Gaussian functions with a constant offset.

$$R_d(\theta) = C + R_p \exp \left\{ \frac{-\|\theta - \theta_{pref}\|^2}{2\sigma_1^2} \right\} + R_n \exp \left\{ \frac{-\|\theta - \theta_{null}\|^2}{2\sigma_2^2} \right\}$$

Where $R_o(\theta)$ is the time-averaged response of neuron to angle of direction θ . Relative magnitude of tuning widths, σ_1 and σ_2 denote the amount of directional selectivity. C is a constant offset.

Parameters are estimated by minimizing squared sum of error. Sum of squared error is defined as:

$$SSE = \sum_{i=1}^N \|R(\theta_i) - R_o(\theta_i)\|^2$$

A gradient descent algorithm finds the optimum parameters by minimizing SSE.

In Figure 3.4 , fit of tuning curves of a complex cell is given. The distinct peak in the orientation tuning curve shows selectivity to orientation θ_{pref} . In the direction tuning curve, peaks of different magnitude shows one direction is more preferred than other. In Figure 3.5 , fit of tuning curves of a complex cell is given. The

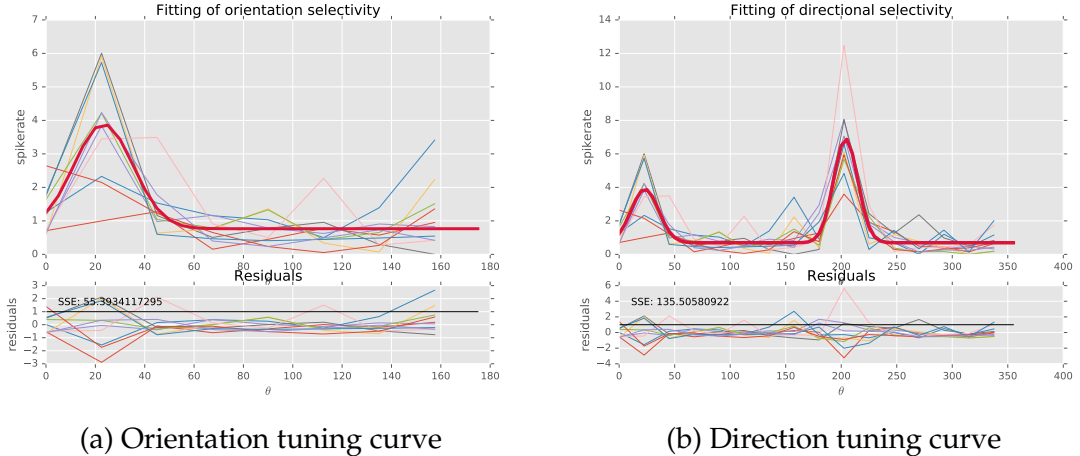


Figure 3.4: Fit of orientation and direction tuning curves of a neuron. The distinct peak in the orientation tuning curve shows selectivity to orientation θ_{pref} . Different σ_1 and σ_2 in direction tuning curve shows direction sensitive cell. - Thus a complex cell

distinct peak in the orientation tuning curve shows selectivity to orientation θ_{pref} . In the direction tuning curve, peaks of same magnitude shows of stimuli direction is irrelevant.

3.3 Finding similarly tuned neurons

Receptive field of a neuron in V1 consists of a subset of neurons in one layer below it. Those neurons in turn have a receptive field. By following layers down, we can find a visual field for each neuron in V1. Orientation selectivity of neurons in V1 detects edges and their orientation in images. By studying similarly tuned neurons, we can get an insight to redundancy of coding and distribution of

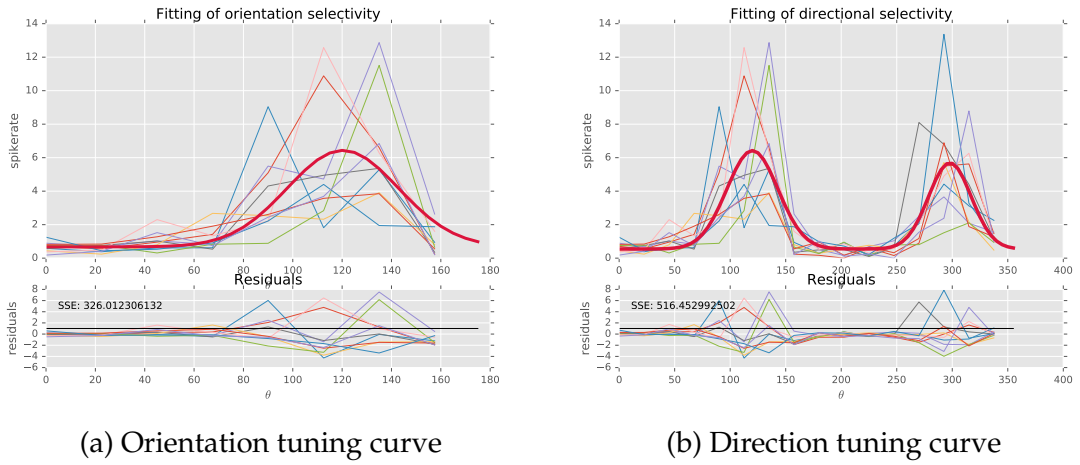


Figure 3.5: Fit of orientation and direction tuning curves of a neuron. The distinct peak in the orientation tuning curve shows selectivity to orientation θ_{pref} . Similar σ_1 and σ_2 in direction tuning curve direction of stimuli is irrelevant. - Thus a simple cell

functionally similar cells in V1.

Similarly tuned cells are expected to have similar response to different stimuli orientations. A high correlation of responses $R(\theta_k)$ to various angle θ_k will represent similarly tuned cells. Even after having same preferred orientations, the neurons could have different degree of selectivity. We would like to find similarly tuned neurons which have an ‘acceptable’ OSI.

Pearson correlation between each pair of neurons in a mice are computed and plotted in Figure 3.6. The neurons in both axes have a decreasing OSI value. The neuron pairs that lie in bottom left of the Figure 3.6 are the ones we have interested. Finally to find neurons that are similarly tuned to a particular neuron, choose the corresponding row and all the neurons in that row having good correlation value and having acceptable OSI are selected. Figure 3.7 shows tuning curves of some neurons retrieved from correlation study.

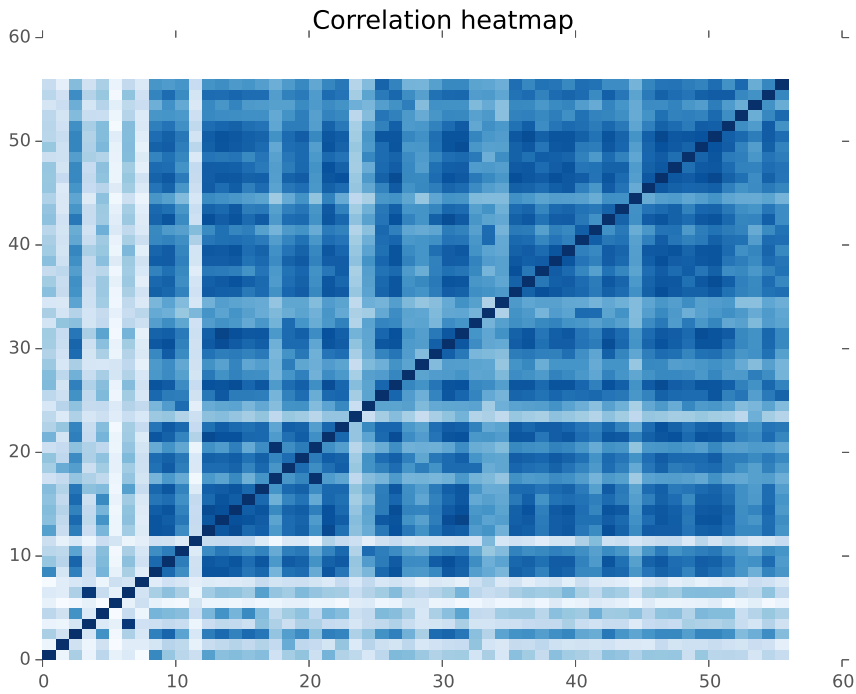


Figure 3.6: Pairwise Pearson correlation of neurons. Both axes are sorted in decreasing order of OSI.

3.4 Study of principal components

Information contained in the visual stimuli reaches V1 after it gets passed through lower layers. Edges and motion of edges in the stimuli are represented by orientation and direction sensitive neurons in V1. Through Principal Component Analysis (PCA) we aim to study the tightness of information representation. A subset of neurons (~ 60) in V1 are sampled at 20Hz for 6 seconds during the experiment. We analyze principal components of the responses to find redundancy in the responses. The number of uncorrelated principal components which capture ‘most’ of the variance in data can determine redundancy.

Principal Component Analysis is an orthogonal transformation of possibly correlated observations to linearly uncorrelated components called principal compo-

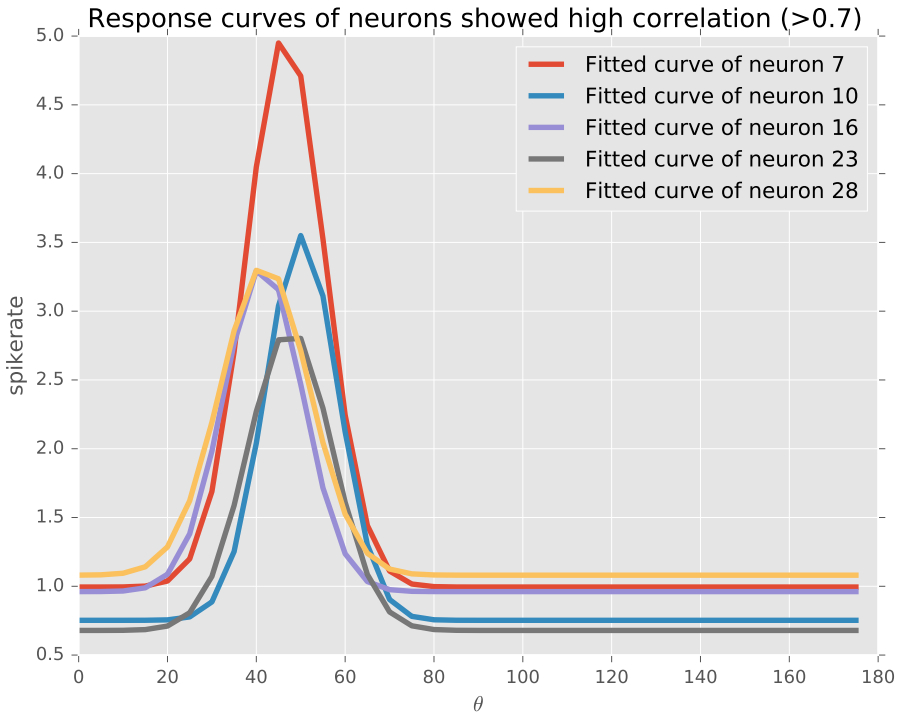


Figure 3.7: Orientation tuning curves of some neurons retrieved from correlation study. All of them have a same preferred orientation.

nents. The principal components are orthogonal because they are the eigenvectors of the covariance matrix, which is symmetric. The first principal component captures largest variance and decreases further. By observing number of components that needs to capture a desired variance, we can tell correlations in the data. Transforming original data to new orthogonal basis gives a representation which has dimension less than or equal to the number of original dimension. Reconstructing original data from subset of principal components also indicates amount of correlation in original data.

Here we take number of neurons as feature dimension. The responses are averages across trials. PCA is done on the data to find ratio between number of principal components and variance explained. Figure 3.8a shows the result for a mouse towards a sinusoidal grating stimuli. The original data was transformed

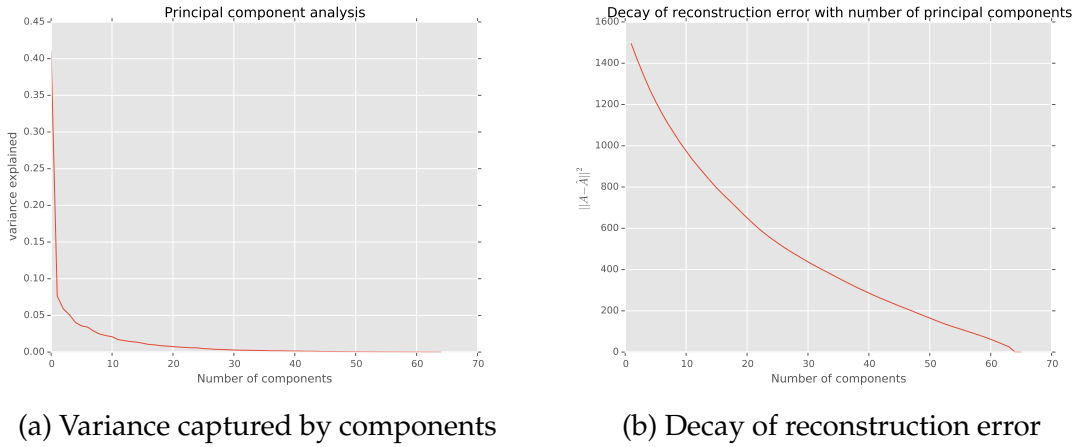


Figure 3.8: Principal Component Analysis of response of neuron to drifting sinusoidal grating stimuli.

to principal components basis with a subset of principal components. Attempting to reconstructing original data from transformed data produces an error. The reconstruction error depends on number of chosen subset of principal components. Figure shows reconstruction error for different number of principal components. As we increase number of principal components, the error decreases. And finally as the number components equals the original feature dimension, reconstruction error vanish.

3.5 Study of Reliability

Information encoding in primary visual cortex is a complex process due to intrinsic neuronal variability. Intertrial reliability of information encoding in neurons is the first step into analyzing coding mechanism of V1. The degree of trial-to-trial variability in a response is commonly measured in terms of reliability. A neuron is said to be reliable if it fires the same number of precisely timed spikes on every repetition of a stimulus [Tiesinga *et al.* [2008]].

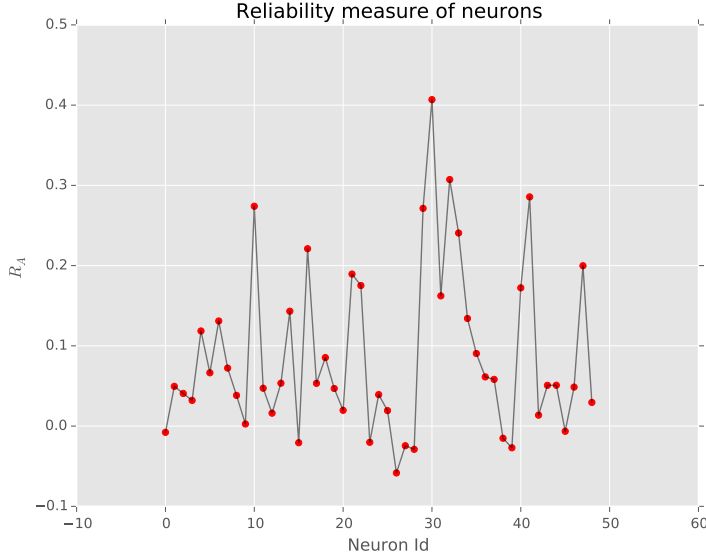


Figure 3.9: Reliability measure R_A for different neurons

The experiment performed measures calcium concentration in neurons rather than spike rate. Trial to trial reliability can be computed using correlation between responses of each trial. When a visual stimuli is presented T times, we can compute response reliability R_A of a neuron to the stimuli A .

$$R_A = \frac{2}{T^2 - T} \sum_{i=1}^T \sum_{j=i+1}^T \rho(f_{i,A}, f_{j,A})$$

where $f_{i,A}$ is the response of neuron to i^{th} trial of movie A and ρ is the Pearson correlation.

The study was done for 48 neurons in a mice and the response reliability is plotted in Figure 3.9 for each neuron. It is evident that response reliability for most of neurons are small. The study shows responses of neurons in V1 are not robust because of intrinsic noise. If the whole sequences is not reliable, could there be subsequences that are reliable? We will explore it in coming chapters by detecting common subsequences.

CHAPTER 4

Searching for Motifs

In Music, motif is a perceivable recurring fragment. They are elementary signatures that repeats to form bigger units. Detecting such motifs in a song tells us more about the song like its melody. In Genetics, motif is a sequence pattern of nucleotides in a longer DNA sequence. From a signal processing perceptive, motifs is a signal segment that recurs in a longer signal. A valid motif should have an ‘acceptable’ length such that it has a significance. Motif analysis is import because in every domain, occurrence of motifs has a meaning to it.

In the experiment, each neuron responses are captured as a time series sampled at 20Hz for 10 seconds. In neuron responses we define a Motif as subsequence of response time series which has the following properties:

- Recurs in the same response signal but in a different part **or**
- Recurs in the response of the same neuron to a different trial **or**
- Recurs in the response of another neuron in the same mouse **or**
- Recurs in the response of neuron in a different mouse **and**
- Has a significant length in time.

Analyzing motifs in neuronal signals will help us understand reliable information representation. Even if two responses of same trial has a long subsequence but not time synchronized, Study of reliability in Section 3.5 will fail as the Pearson correlation coefficient will output a small value. Motivic analysis can detect such subsequences even if they are time shifted.

Study of motifs across two different neurons within a mouse can explain correlation between two neurons. Correlated neurons can represent neuronal interconnections. Correlated and synchronous activity in populations of neurons has been observed in many brain regions and has been shown to play a crucial role in cortical coding, attention, and network dynamics [Rosenbaum *et al.* [2014]]. Studying correlations between neurons is again not effective if their responses are time separated as Pearson correlation will fail. Analyzing motifs across neurons will be a better way to study neuronal correlations.

Motifs found in neurons from two *different* mice will represent similar biological process both the neurons undergoes. As the motifs found cannot be due to interconnections, they are due to same activation mechanism of neurons. In this case, we would expect a small motif compared to motifs found within mouse.

In this chapter, we will analyze the presence of motifs in neuronal signals. The presence of motifs will motivate us to extract the motifs and their significance.

4.1 Cross-Correlation Function

Cross correlation is a measure of similarity between two signals as a function of lag of one signal relative to the other. It is commonly used for searching a short query sequence in a large reference sequence. The function calculates sliding dot product at various lags. For discrete signals, cross correlation is defined as:

$$(f \star g)[n] \stackrel{\text{def}}{=} \sum_{m=-\infty}^{\infty} f^*[m] g[m+n].$$

Searching for a motif using correlation function is possible if we already have a subsequence that we suspect as a motif. To visualize correlation function in query search, we will manually select a subsequence and search for its occurrences in a neuronal response signal. For the scope of this chapter, we take a subsequence from the response of a ‘template neuron’ and search for its occurrences in response of a ‘target neuron’.

Trial averaged responses of template and target neurons are taken, then a subset of former is extracted using parameters frame ending and frame width. This subsequence is compared with target sequence as a function of lag. Figure 4.1 shows Cross-Correlation function between a target neuron response and a manually chosen subsequence from template neuron. This study is not effective as we

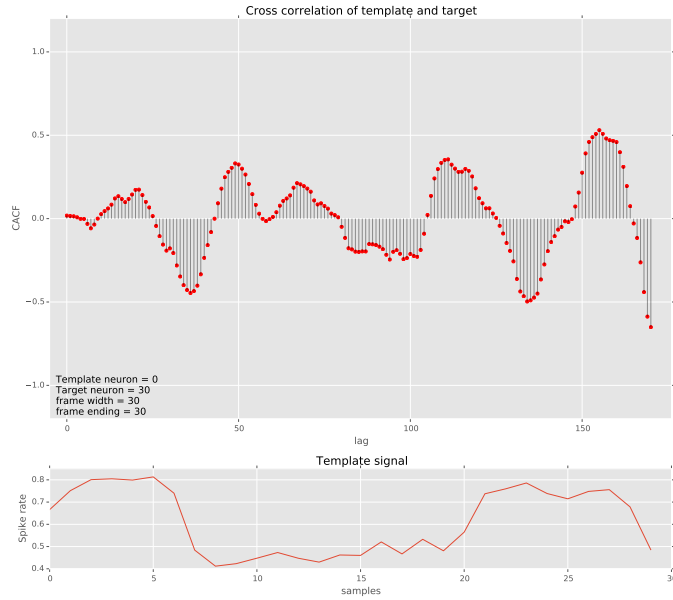


Figure 4.1: Cross-Correlation function between a target neuron response and a manually chosen subsequence from template neuron.

do not know what to search for. Manually selecting a subsequence is inefficient and selected subsequence does not guarantee to be valid motif.

4.2 ACFGram

A spectrum describes a signal in terms of energy spread over its frequency components. A spectrogram does exactly the same but also takes another time into consideration. Computing spectrogram is done by first making chunks/frames of time-domain signal which usually overlap. Magnitude of Fourier transform of each frame is computed to form magnitude spectrum of that frame. These frame spectra are stacked horizontally in increasing order of frame ending time to form a spectrogram. This enables us to study the change of spectra with time.

We formulate an analogous visualization of Cross-Correlation function where the template signal changes in each frame. A frame is a subsequence of original signal with a width and frame ending parameter. Changing the frame ending successively will return overlapping frames having same width. Figure 4.2 shows how a frame from template signal is selected. Cross-Correlation of extracted

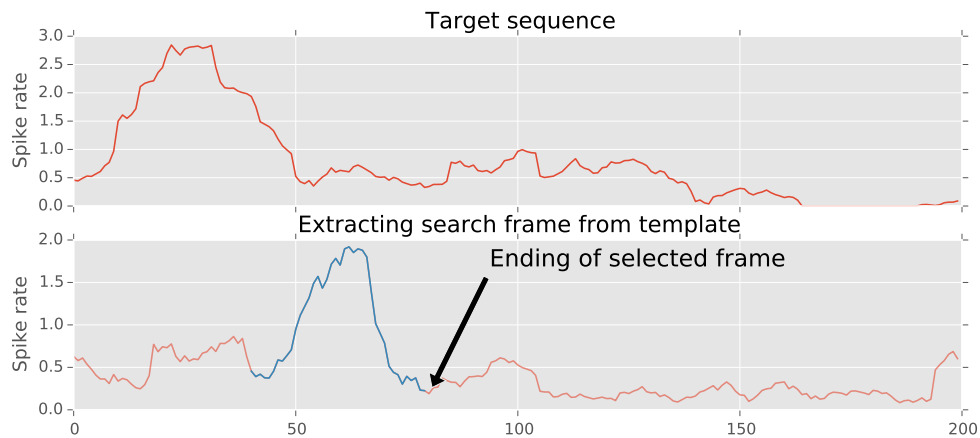


Figure 4.2: Extracting frame from template based on frame width and ending.

frame and target signal at various lags are computed. Next frame is extracted by incrementing frame ending parameter. The process is then repeated for the next frames. Cross-Correlation function of each frame is then stacked horizontally to

form a temporal dimension. We call the resulting Time Vs Lag Vs Cross-Correlation function as ACFGram. In the previous study In Section 4.1 we varied frame width and frame ending manually to extract a signal subsequence and then queried it in target signal. ACFGram removes frame ending parameter. Existence of motifs will be clear if we iterate frame width. The study was conducted across trials of same neuron and across different neurons.

The Figure 4.3b shows ACFGram plots for template and target responses from same neuron. The study aim to find presence of repeating subsequence within a neuron's response. The length of suspected motif is varied as a parameter. For a small frame width (~ 15) the estimation of Cross-Correlation function is poor. Also such a small subsequence is not significant enough to be considered as a motif. As we Increase the frame width, repeating patterns are found which indicates the presence of repeating subsequence. The Figure 5.7b shows ACFGram plots for

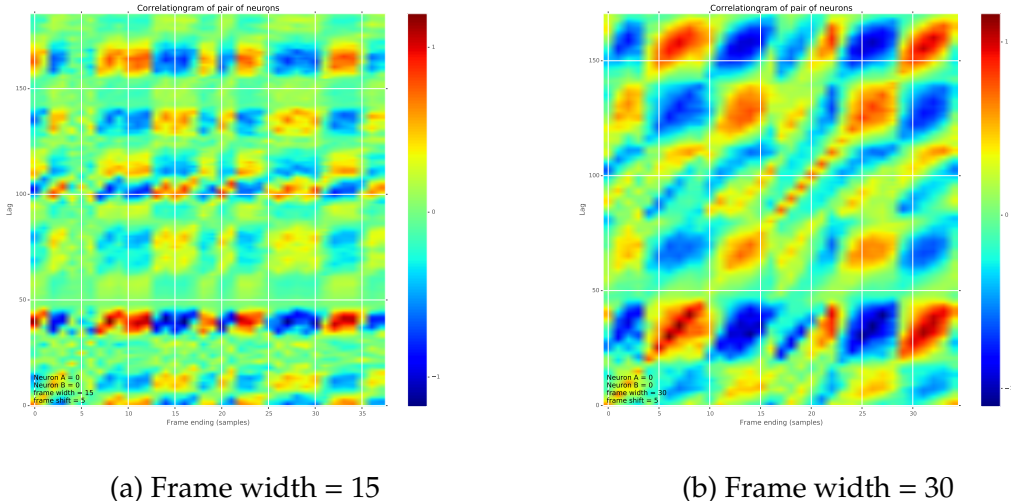


Figure 4.3: ACFGram plots for template and target responses from same neuron.

two different neuron responses. Motifs across neurons are studied for finding a better correlation metric. For different frame widths, responses indicate presence of motifs across neurons. The approximate length of motifs is more than 2 seconds,

which is significant. Importantly, more or less any pair of neurons taken from the sampled set of 65 neurons from each mouse exhibited the presence of motifs. This indicates the inter neuronal correlation. This supports the claim that information in V1 is coded in population by inter-neuronal correlations. The search for the

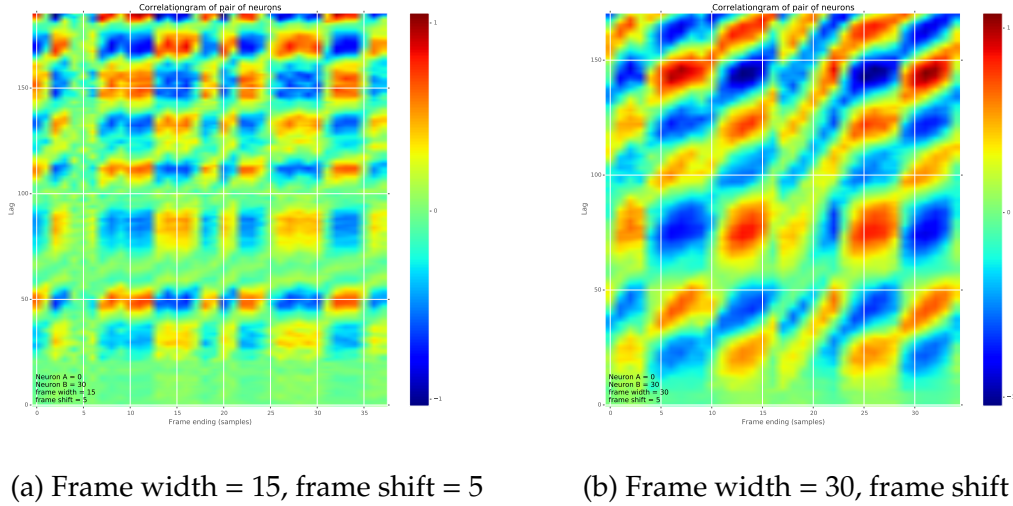


Figure 4.4: ACFGram plots for template and target responses from different neurons.

presence of motifs in primary visual cortex succeeded in with experimentally verifying rough common subsequences of significance (> 2 seconds) exists in neuronal responses. This motivates us to find the longest motifs you can find between two neurons. Also till now we used Pearson correlation as a measure of similarity. We look into rough measures of similarity and longest common subsequence in the next chapter.

CHAPTER 5

Rough Longest Common Subsequence (RLCS)

Having established existence of motifs in neuronal responses, A robust algorithm to extract best possible motifs from two signals is required. As a longer motif has more significance in the context, an algorithm which produce longest common subsequence is desirable. Longest Common Subsequence (LCS) is a classical problem in query string matching, data comparison and Bio-informatics. We will eventually look into an adapted LCS problem which can be used to match signals called Rough Longest Common Subsequence (RLCS).

5.1 Longest Common Subsequence (LCS)

A subsequence of a string S is a set of characters that appear from left to right in original string S but not necessarily consecutive. There will be more than one subsequence for any string with length greater than unity. For two strings S_1 and S_2 , the common entries in sets of substrings of each strings are called common subsequences of S_1 and S_2 . Among the common subsequences, the subsequence with maximal length is called Longest Common Subsequence.

Some examples of LCS are given in Table 5.1. Note that there can be more than one LCS for two strings.

LCS problem can be defined formally for two subsequences $X = (x_1, x_2 \dots x_m)$

String 1 - S_1	String 2 - S_2	$LCS(S_1, S_2)$
ABCDGH	AEDFHR	ADH
AGGTAB	GXTXAYB	GTAB
AGCAT	GAC	AC, GC and GA
BACDB	BDCB	BCB

Table 5.1: Some examples of LCS in string comparison

and $Y = (y_1, y_2 \dots y_n)$ as

$$LCS(X_i, Y_j) = \begin{cases} & \text{if } i = 0 \text{ or } j = 0 \\ LCS(X_{i-1}, Y_{j-1}) \cup x_i & \text{if } x_i = y_j \\ \text{longest}(LCS(X_i, Y_{j-1}), LCS(X_{i-1}, Y_j)) & \text{if } x_i \neq y_j \end{cases}$$

Where $X_i = (x_1, x_2 \dots x_i)$ and $Y_j = (y_1, y_2 \dots y_j)$.

LCS problem has an optimal substructure- the problem can be broken down into subproblems of similar kind. As the problem also has overlapping subproblems, a Dynamic Programming approach is used to find the LCS. Running time of the dynamic programming approach is $O(nm)$ where n and m are the lengths of strings.

5.2 RLCS

LCS problem can be adapted for signal matching. Instead of equality, a rough distance measure is used. If the distance between samples is less than a threshold, they are considered a match. It is not desirable just to optimize the length of subsequence in signals as the gaps between selected samples can cause false alarms. Dynamic Programming optimization has to be penalizing gaps and motivating matches. The rest of the problem and the solution remains similar to LCS problem and similar Dynamic Programming approach can solve the problem efficiently.

Modified LCS problem with rough comparison is stated below. The RLCS of two input sequences $X = \langle x_1, x_2, \dots, x_m \rangle$ and $Y = \langle y_1, y_2, \dots, y_n \rangle$ is obtained by maximizing the score value S .

$$S(X_i, Y_j) = \begin{cases} 0 & \text{if } i = 0 \text{ or } j = 0 \\ S(X_{i-1}, Y_{j-1}) + x_i & \text{if } dist(x_i, y_j) < \tau_{dist} \\ \max(S(X_i, Y_{j-1}), S(X_{i-1}, Y_j)) & \text{if } dist(x_i, y_j) > \tau_{dist} \end{cases}$$

Where $X_i = \langle x_1, x_2, \dots, x_i \rangle$ and $Y_j = \langle y_1, y_2, \dots, y_j \rangle$.

Various context uses different distance measures for comparing samples. Manhattan distance (city block distance) of notes is used in context of music matching [Lin *et al.* [2011]]. In a work on verification of Raga in Carnatic music [Dutta *et al.*], a domain specific similarity measure is used. RLCS on neuronal signals in this work uses normalized Euclidean distance for checking similarity.

$$dist(x_i, y_i) = (x_i - y_i)^2$$

Distances are normalized from 0 to 1 by performing:

$$dist(x_i, y_i) = \frac{dist(x_i, y_i) - minDist}{maxDist - minDist}$$

Where $minDist$ is the minimum pairwise distance and $maxDist$ is the maximum pairwise distance.

Most important part of RLCS is the adapted score update rules. In the classical LCS problem, the gaps between the selected subsequence was not considered; Instead only the length of the subsequence was of consideration. But in signals,

having a gap in between will give poor signal match. So it is important to penalize the gaps and reward matches. The following score update rules penalizes gaps in subsequence and awards positive score for matches.

1. Score update for a match. $dist(x_i, y_j) < \tau_{dist}$

$$score(i, j) = score(i - 1, j - 1) + 1 - \frac{dist(x_i, y_j)}{\tau_{dist}}$$

This case happens when a match is found. The score should be rewarded with a positive value. The maximum awarded score is 1 for an exact sample match and minimum score given is 0 for when the distance equals threshold. The closer the samples, more the score.

2. Score update for a mismatch. $dist(x_i, y_j) > \tau_{dist}$

$$score(i, j) = score(i - 1, j - 1) - \delta$$

We allowed any number of gaps in a string LCS problem. But in the case of signals, we cannot allow large gaps as it would produce false alarms. We penalize each mismatching samples with a constant score δ .

The problem is then recursively solved using Dynamic Programming algorithm which will provide us with a 2-D score matrix. The Dynamic programming algorithm for input sequences $X = < x_0, x_1, \dots, x_{m-1} >$ and $Y = < y_0, y_1, \dots, y_{n-1} >$ is explained in

Backtracking through score matrix will gives us the Longest Common Subsequence. As we have been penalizing gaps, there will be points in the track where score is zero. For each sample match we had increased score and decreased for gaps. So the zero will mean that there are enough mismatches to balance the positive score created by matches. This lets us identify the boundary of a subsequence. A number of subsequences could be extracted by cutting at points where score goes zero. This set of subsequences are called **Longest Common Subsequence Set** (LCSS) [Dutta *et al.*]. Algorithm ** explains backtracking to extract the LCSS.

Algorithm 1 Dynamic Programming algorithm for RLCS ***

```
1: function RLCS( $X, Y, \tau_{dist}, \delta$ )
2:    $m \leftarrow$  length of  $X$ 
3:    $n \leftarrow$  length of  $Y$ 
4:    $p \leftarrow \min(m, n)$ 
5:   for  $i = 0; i < m; i++$  do
6:     for  $j = 0; j < n; j++$  do
7:        $dist(i, j) \leftarrow euclideanDistance(x_i, y_j)$ 
8:        $\text{minDist} \leftarrow \min(dist)$                                  $\triangleright$  For normalization
9:        $\text{maxDist} \leftarrow \max(dist)$                                  $\triangleright$  For normalization
10:
11:       $\text{cost} \leftarrow zeros(m + 2, n + 2)$                                  $\triangleright$  For storing running score
12:       $\text{score} \leftarrow zeros(m + 2, n + 2)$                                  $\triangleright$  For storing score
13:       $\text{diag} \leftarrow zeros(m + 2, n + 2)$                                  $\triangleright$  For backtracking
14:       $\text{partial} \leftarrow zeros(m + 2, n + 2)$                                  $\triangleright$  For storing partial scores.
15:
16:      for  $i = 0; i < m; i++$  do
17:        for  $j = 0; j < n; j++$  do
18:           $d \leftarrow (dist(i, j) - \text{minDist}) / (\text{maxDist} - \text{minDist})$        $\triangleright$  Normalize
19:          if ( $d < \tau_{dist}$ ) then
20:             $\text{diag}(i, j) \leftarrow ' \nearrow '$                                  $\triangleright$  Path to travel while backtracking
21:             $\text{cost}(i, j) \leftarrow \text{cost}(i - 1, j - 1) + (1 - d/\tau_{dist})$ 
22:             $\text{score}(i, j) = \text{score}(i - 1, j - 1)$ 
23:          else if  $\text{cost}(i - 1, j) > \text{cost}(i, j - 1)$  then
24:             $\text{diag}(i, j) \leftarrow ' \uparrow '$ 
25:             $\text{cost}(i, j) = \text{cost}(i - 1, j) - \delta$                                  $\triangleright$  Penalize
26:          if  $i > stringlen$  then return false
27:           $j \leftarrow patlen$ 
28:        loop:
29:          if  $string(i) = path(j)$  then
30:             $j \leftarrow j - 1.$ 
31:             $i \leftarrow i - 1.$ 
32:            goto loop.
33:            close;
34:           $i \leftarrow i + \max(delta_1(string(i)), delta_2(j)).$ 
35:        goto top.
```

Algorithm 2 Dynamic Programming algorithm for RLCS ***

```
1: function RLCS( $X, Y, \tau_{dist}, \delta$ )
2:    $m \leftarrow$  length of  $X$ 
3:    $n \leftarrow$  length of  $Y$ 
4:    $p \leftarrow \min(m, n)$ 
5:   for  $i = 0; i < m; i++$  do
6:     for  $j = 0; j < n; j++$  do
7:        $dist(i, j) \leftarrow euclideanDistance(x_i, y_j)$ 
8:        $\text{minDist} \leftarrow \min(dist)$                                  $\triangleright$  For normalization
9:        $\text{maxDist} \leftarrow \max(dist)$                                  $\triangleright$  For normalization
10:
11:       $\text{cost} \leftarrow zeros(m + 2, n + 2)$                            $\triangleright$  For storing running score
12:       $\text{score} \leftarrow zeros(m + 2, n + 2)$                            $\triangleright$  For storing score
13:       $\text{diag} \leftarrow zeros(m + 2, n + 2)$                            $\triangleright$  For backtracking
14:       $\text{partial} \leftarrow zeros(m + 2, n + 2)$                           $\triangleright$  For storing partial scores.
15:
16:      for  $i = 0; i < m; i++$  do
17:        for  $j = 0; j < n; j++$  do
18:           $d \leftarrow (dist(i, j) - \text{minDist}) / (\text{maxDist} - \text{minDist})$      $\triangleright$  Normalize
```

5.2.1 Motivic analysis of Neuronal signals with RLCS

Having established presence of motifs in neuronal responses, we use Rough Longest Common Subsequence (RLCS) algorithm to find the ‘best’ motifs from a signal processing point of view. Penalizing the gaps makes RLCS a good signal matching algorithm.

The experiment was conducted on responses of neurons from V1 of 11 mice to different visual stimuli. Each signal is sampled at 20 Hz and last for 10 seconds. The study is split into different sections based on which neurons the signals come from.

Motifs in responses of a neuron to different trials

The signals from a neuron’s response to different trials of same stimuli are passed to RLCS algorithm to detect motifs. The Figure 5.1 shows score matrix obtained

after RLCS. The effect of τ_{dist} was experimentally studied and fixed at 0.005. For τ_{dist} above 0.001, false alarms increased. Decreasing threshold caused bad detection rate. The desired motif takes a path through the score matrix. The diagonal shifts in the score path are sample matches - as a result of that we can see the increase in score. Shifting to right or top denotes a gap in the subsequence. As mismatches cause penalty, the score will decrease. When enough mismatches to compensate the total positive score are encountered, The score will become zero. Such points on the backtrack path having zero score mark boundaries of subsequences.

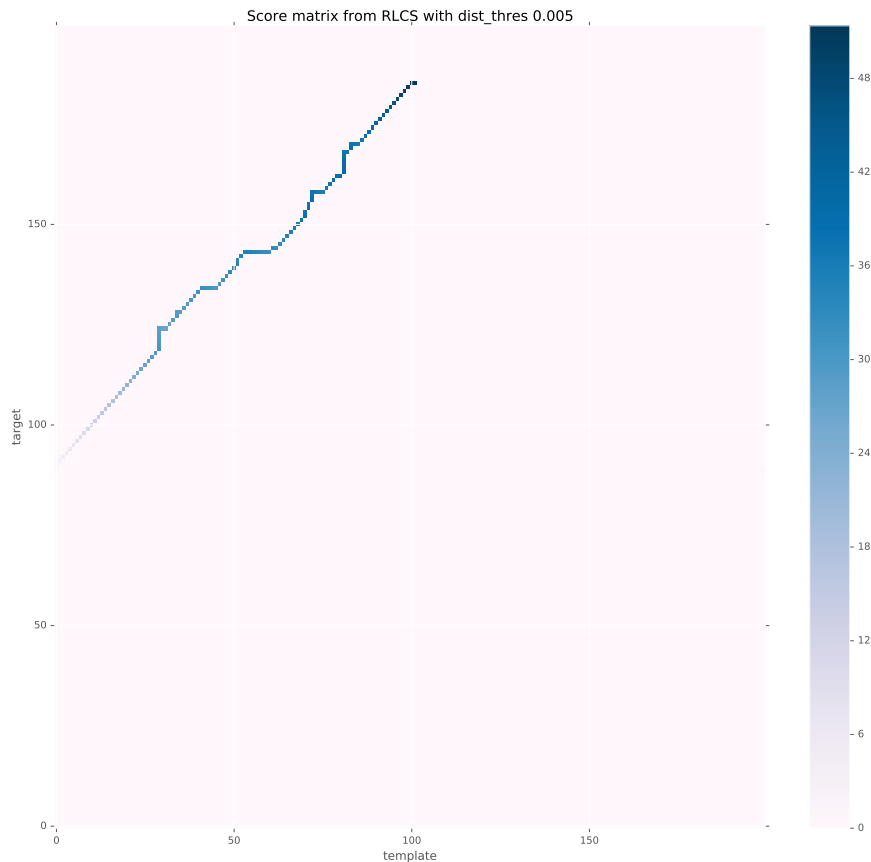


Figure 5.1: Score matrix from RLCS of responses a neuron to different trials.

The Figure 5.2 shows a motif from the responses of a neuron to different trials. The signal retrieved shows good similarity. At 20Hz sampling frequency, the motif

lasts more than 6 seconds. Which is a significant time for two neurons to have very similar response. Also, similar phenomena occurs in each neuron we studied.

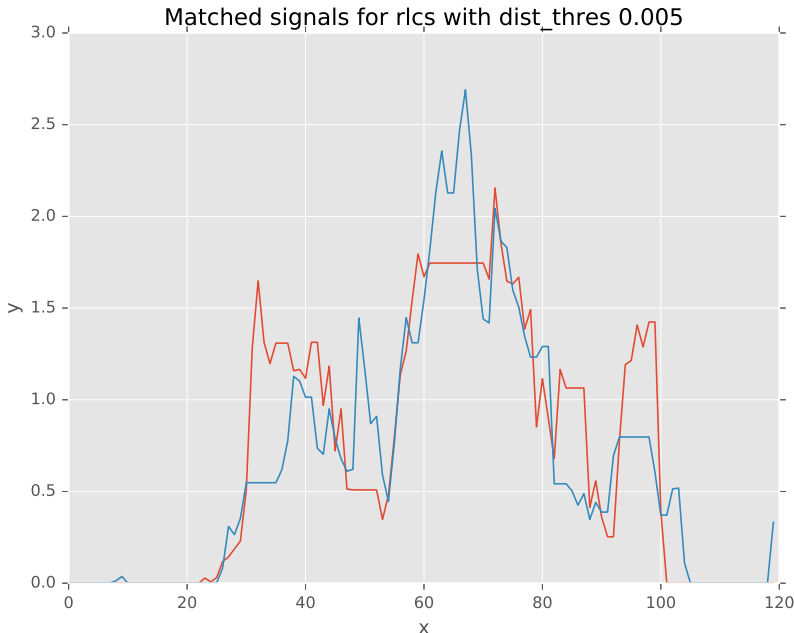


Figure 5.2: Extracted motif (longest) from responses a neuron to different trials.

Motifs in responses of two neurons in a mice

Responses of two neurons to same visual stimuli are analyzed for motifs. Both neurons were sampled simultaneously during experiment. The Figure 5.3 shows score matrix and Figure 5.4 shows longest motif spotted. Note that in this case, motif has a duration of 7 seconds. In the score matrix, two disconnected paths can be found. Each one of these correspond to a common subsequence. Set of such subsequences are LCSS. Motifs across mice have an average duration about 3 seconds. More or less any two neurons taken for study, motifs of length > 2 seconds were spotted. This shows correlation in responses of neurons. In some cases, the length of motif exceeded 6 seconds.

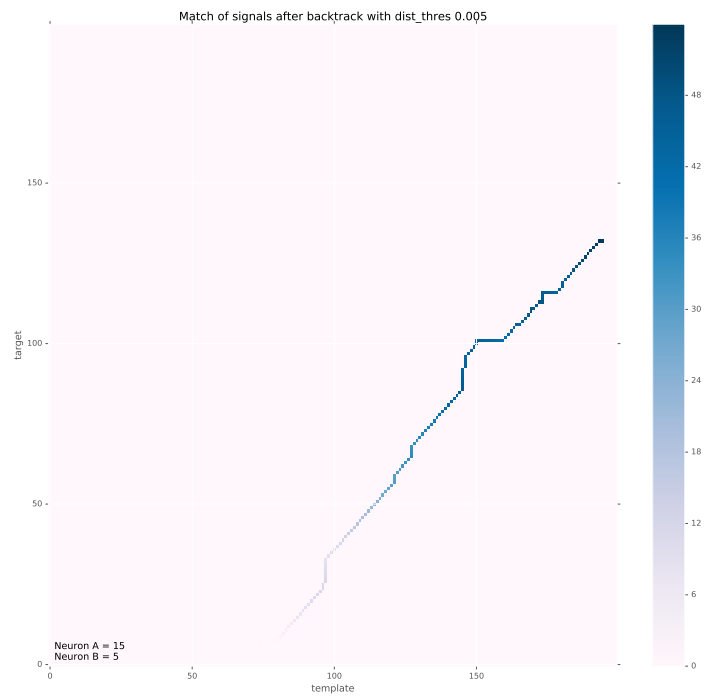


Figure 5.3: Score matrix from RLCS of responses of two neurons in a mouse.

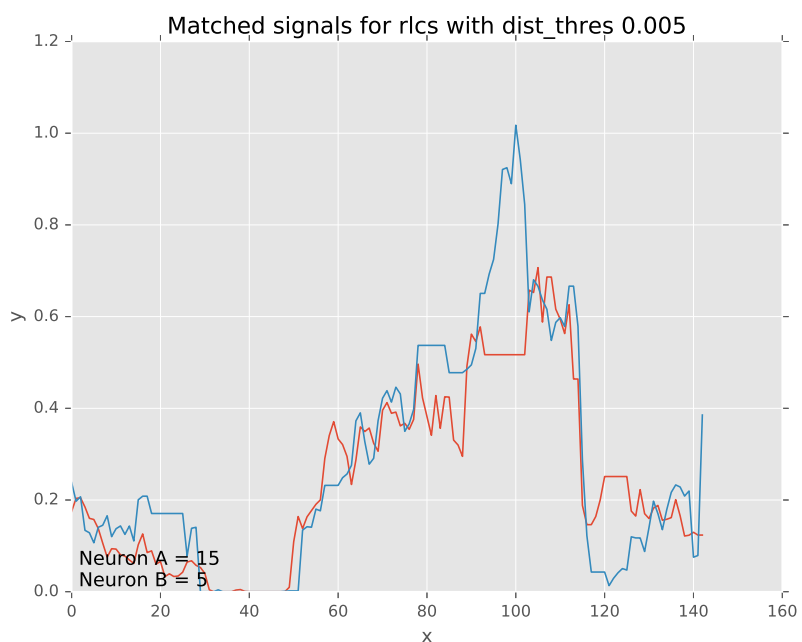


Figure 5.4: Extracted motif (longest) from responses of two neurons in a mouse.

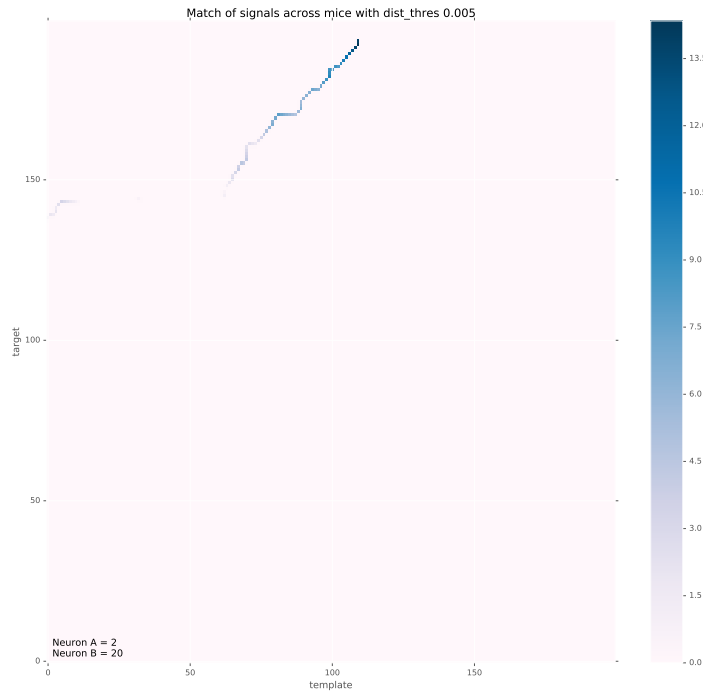


Figure 5.5: Score matrix from RLCS of responses of two neurons in a mouse.

Motifs in responses of neurons across different mice

Two neurons across two mice were taken for study. As the neurons does not have any interconnections, the motifs are expected to have less duration if at all they exists. The study proved that motifs across mice occurs very less frequent than previous cases. Even when they exists, they have short duration ~ 2 seconds. Motifs across mice could be caused by similar activation mechanism of neurons. This explains absence of long motifs across mice and presence of short subsequences. Exceptionally in some cases motifs of duration ~ 4 seconds were spotted across mice. Figure 5.5 and Figure 5.6 shows score matrix and extracted motif from responses of two neurons across mice. More plots of score matrix and motifs are in Appendix A.

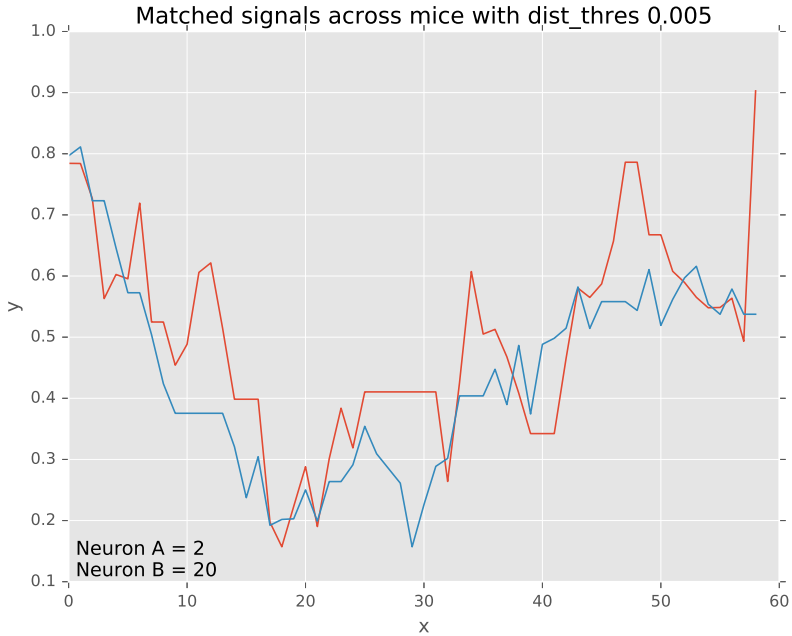


Figure 5.6: Extracted motif (longest) from responses of two neurons in a mouse.

5.2.2 Normalized RLCS score as a correlation measure

We have seen RLCS was very effective in query search, signal matching and correlation study even when classical correlations metric Pearson correlation coefficient failed to detect correlation. As the information encoding in V1 largely depend on population of neurons and their inter-correlations, A robust measure of signal correlations needs to be used for analysis. We explore the possibility of normalized RLCS score between two signals as a robust correlation metric.

The sum of RLCS scores contain information about how close the matched samples are, how long is the detected subsentence, how much gaps they have in between samples. This brings the consideration of using RLCS score as correlation measure. But to compare two scores, we need it to be normalized. We use standard z-normalization In which average score will be transformed to zero; all the scores above mean gets a positive score and every score below mean score gets a negative

score. Please note that this is effective only when a large dataset is used as mean and standard deviation needs to be estimated. The standard z - score of a raw RLCS score s is

$$z = \frac{x - \mu}{\sigma}$$

Where $s = \sum_{i,j} \text{score}(i, j)$ is the raw RLCS score. μ is the mean and σ is the standard deviation of the population of scores.

As a demonstration, Figure shows two signals which have a low Pearson correlation $\rho = 0.18$ and good RLCS score. The extracted subsequence shows good similarity on ~ 140 samples which was not detected by Pearson correlation. The score plot shows that many of the matches were not on the diagonal line. Pearson correlation is reliable only to detect similarities in the diagonal line of score matrix.

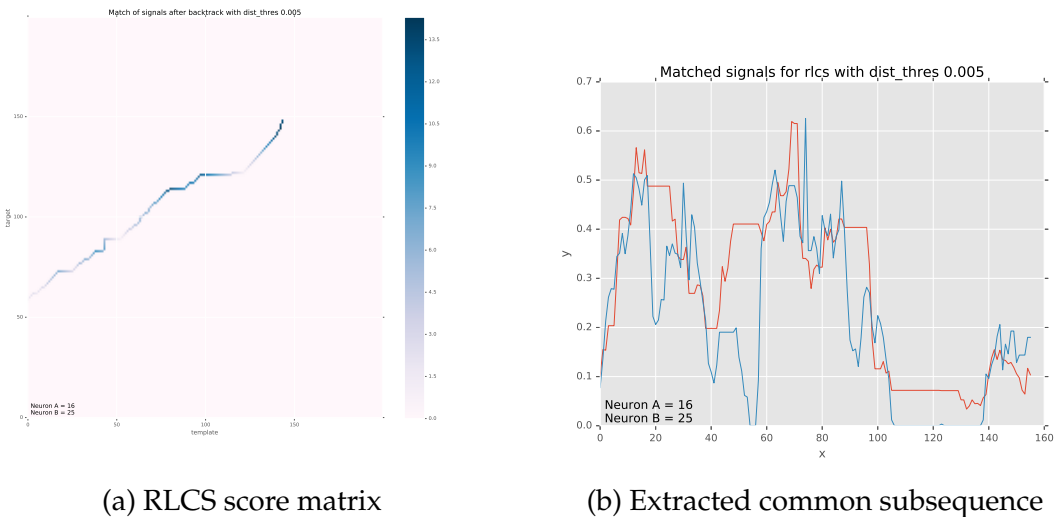


Figure 5.7: Demonstration of RLCS score's dominance over Pearson correlation as a metric of similarity. RLCS analysis of two signals having low Pearson correlation. Extracted common subsequence was not detected by Pearson correlation.

CHAPTER 6

Inferences and Future work

APPENDIX A

More RLCS plots

REFERENCES

- Bear, M., B. Connors, and M. Paradiso,** *Neuroscience*:: Neuroscience: Exploring the Brain. Lippincott Williams & Wilkins, 2007. ISBN 9780781760034. URL <https://books.google.co.in/books?id=75NgwLzueikC>.
- Dutta, S., K. S. PV, and H. A. Murthy** (). Raga verification in carnatic music using longest common segment set.
- Hubel, D., Eye, Brain, and Vision.** Scientific American Library Series. Henry Holt and Company, 1995. ISBN 9780716760092. URL <https://books.google.co.in/books?id=2Id9QgAACAAJ>.
- Lin, H.-J., H.-H. Wu, and C.-W. Wang** (2011). Music matching based on rough longest common subsequence. *J. Inf. Sci. Eng.*, **27**(1), 95–110.
- Rikhye, R. V. and M. Sur** (2015). Spatial correlations in natural scenes modulate response reliability in mouse visual cortex. *The Journal of Neuroscience*, **35**(43), 14661–14680.
- Rosenbaum, R., T. Tchumatchenko, and R. Moreno-Bote,** *Correlated neuronal activity and its relationship to coding, dynamics and network architecture*:: Frontiers Research Topics. Frontiers E-books, 2014. ISBN 9782889193578. URL <https://books.google.co.in/books?id=AQNdBgAAQBAJ>.
- Tiesinga, P., J.-M. Fellous, and T. J. Sejnowski** (2008). Regulation of spike timing in visual cortical circuits. *Nature reviews neuroscience*, **9**(2), 97–107.
- Vogelstein, J. T., A. M. Packer, T. A. Machado, T. Sippy, B. Babadi, R. Yuste, and L. Paninski** (2010). Fast nonnegative deconvolution for spike train inference from population calcium imaging. *Journal of neurophysiology*, **104**(6), 3691–3704.